

Synthesis and characterization of novel poly(aryleneethynylene)s derived from squaraines for photovoltaic applications

Wei Zhang · Feng Tao · Kai-ge Meng ·
Zheng Wang · Long-yi Xi · Ying Li ·
Qing Jiang

Received: 15 February 2011 / Accepted: 14 March 2011 / Published online: 31 March 2011
© Springer Science+Business Media, LLC 2011

Abstract Two novel π -conjugated polymers composed of alkyl carbazole/dialkoxyphenylene and squaraine units were synthesized by Sonogashira cross-coupling reactions. The structures and properties of these copolymers were characterized using FT-IR, NMR, UV–Vis, gel permeation chromatography and cyclic voltammetry (CV). Both polymers possess adequate thermal stability and exhibit good solubility in common organic solvents such as chloroform, THF, and toluene. The polymer films show intense and broad visible and near IR absorption with the long wavelength absorption maximum peaks of 796 and 851 nm for **P**₁ and **P**₂, respectively, which are apparently red-shifted compared with poly(phenyleneethynylene). CV studies reveal that the band gaps of these copolymers are about 1.45 eV, implying that the resulted polymers may be promising candidates for solar cells.

Introduction

Solar cells based on conjugated polymers have attracted continuing attention in recent years because of their unique advantages, such as low cost, light weight, and good compatibility with the roll-to-roll process for making flexible large area devices [1–6]. Development in this area has grown rapidly, and power conversion efficiencies (PCEs) of 6–7% have been reported in recent years [7, 8]. By exploiting better materials and optimizing the device architectures, further improvement may be achieved.

Poly(aryleneethynylene)s (PAEs) have attracted considerable interest due to their potential use in organic optoelectronic materials [9, 10]. Such polymers are chemically stable and easily accessed via Sonogashira cross-coupling methodology. However, these polymers possess relatively large band gaps between the highest occupied molecular orbital (HOMO) and the lowest unoccupied molecular orbital (LUMO), which may lead to unsatisfactory PCEs in photovoltaic devices [11]. To tune the electronic characteristics of the conjugated system, modification of the conjugation backbone is most effective.

Squaraines, 1,3-disubstituted derivatives of squaric acid, show intense and sharp absorption bands in the visible and near IR regions, which render them attractive for dye-sensitized solar cells (DSSCs) and the bulk-heterojunction organic photovoltaic (BHJ-OPV) solar cells [12, 13]. Ajayaghosh [14, 15] reported a series of extremely low optical band gap polymers with excellent absorption in the near IR region based on squaraines, suggesting that the polymers may have low band gaps and good optical absorption properties by incorporation of squaraine units into their main chains.

Herein, we designed and synthesized two novel donor–acceptor PAEs (**P**₁, **P**₂) based on alkyl carbazole/dialkoxyphenylene as bridging unit and appropriate designed squaraine as the electron-accepting building block. The polymers have a long donor such as carbazole, alkoxy benzene, and pyrrole in the alternating main chain (⋯A-DDDD-A-DDDD⋯). This strategy may manipulate the electronic structure (HOMO/LUMO levels) through the intramolecular charge transfer (ICT) happening in the D–A systems [16, 17]. Moreover, different alkyl side chains were attached onto the conjugated polymers to achieve good solubilities and high molecular weights. The electrochemical and photophysical properties were investigated, and the

W. Zhang · F. Tao · K. Meng · Z. Wang · L. Xi · Y. Li (✉) · Q. Jiang
College of Chemistry, Sichuan University, Chengdu 610064,
China
e-mail: profliying@sina.com

results suggested that the copolymers may be suitable candidates for solar cells due to their broad optical absorption, relatively low band gaps and good thermal stability.

Experimental

Materials

Unless otherwise indicated, all starting materials were obtained from Aldrich and were used without purification. All the solvents were properly purified before use. Pyrrole-2-carboxaldehyde (**1**) [18], *N*-hexadecylpyrrole-2-carboxaldehyde (**2**) [19], 2-bromohydroquinone (**3**) [20], 1-bromo-2,5-dioctyloxybenzene (**4**) [20], 1-bromo-4-bromomethyl-2,5-dioctyloxybenzene (**5**) [20], 4-bromo-2,5-dioctyloxybenzylidethylphosphonate (**6**) [20], *N*-(2-ethylhexyl)-2,7-dibromocarbazole (**8**) [21], 2,5-dioctyloxy-1,4-bis(3-methyl-3-hydroxybut-1-ynyl)benzene (**11**) [22], and 2,5-dioctyloxy-1,4-diethynylbenzene (**12**) [22] were prepared following the published procedures.

Measurements

¹H and ¹³C NMR spectra were recorded on Bruker DRX 400 spectrometer with tetramethylsilane as an internal reference. The FT-IR spectra were obtained on a Perkin-Elmer 2000 infrared spectrometer as KBr pellets. Thermal gravimetric analysis (TGA) was performed on Perkin-Elmer series 7 thermal analysis system under nitrogen at a heating rate of 10 °C min⁻¹. Number-average (M_n) and weight-average (M_w) molecular weights and polydispersity indices (M_w/M_n) of the polymers were measured on a PL-GPC model 210 chromatograph at 25 °C using THF as the eluent and standard polystyrene as the reference. UV–Vis spectra in solutions and thin films were taken on a Shimadzu UV2100 UV–Vis recording spectrophotometer. Differential scanning calorimetry (DSC) measurements were performed on a Perkin-Elmer DSCII under nitrogen at a heating rate of 10 °C min⁻¹. The cyclic voltammograms were recorded on a computer-controlled EG&G potential/galvanostat model 283 at room temperature. The thickness of films was measured by a Dektak surface profilometer.

Synthesis of monomers

(E)-1-bromo-4-[2-(1-hexadecylpyrrole-2-yl)vinyl]-2,5-dioctyloxybenzene (**7**)

A solution of *t*-BuOK (1.19 g, 10.65 mmol) in anhydrous THF (10 mL) was added dropwise at ambient temperature under nitrogen to a mixture of 4-bromo-2,5-dioctyloxybenzyl-

diethylphosphonate (**1**) (2.00 g, 3.55 mmol) and *N*-hexadecylpyrrole-2-carboxaldehyde (**2**) (1.13 g, 3.55 mmol) in 20 mL anhydrous THF. After the sample was refluxed for 12 h, the reaction mixture was cooled to room temperature, and THF was removed under reduced pressure. The residue was neutralized with 5% hydrochloric acid and extracted with chloroform. The extraction was washed with water, saturated NaHCO₃, and brine, then dried over anhydrous MgSO₄ and concentrated. The residue was purified by column chromatography (silica gel, hexane/dichloromethane, 5:1) to afford the product as white solid (1.94 g, 2.66 mmol, 75%). ¹H NMR (400 MHz, CDCl₃): δ = 0.81 (m, 9H), 1.17–1.23 (m, 40H), 1.35–1.48 (m, 6H), 1.67–1.79 (m, 6H), 3.87 (t, *J* = 12.4 Hz, 4H), 3.94 (t, *J* = 12.8 Hz, 2H), 6.09 (s, 1H), 6.41 (s, 1H), 6.60 (s, 1H), 6.91 (s, 1H), 6.96–6.98 (m, 3H). ¹³C NMR (400 MHz, CDCl₃): δ = 151.07, 149.73, 131.73, 127.13, 122.66, 120.79, 118.72, 117.54, 112.56, 110.81, 108.22, 106.78, 70.46, 69.42, 47.12, 31.94, 31.85, 31.60, 29.71, 29.68, 29.62, 29.58, 29.43, 29.38, 29.29, 26.88, 26.18, 26.06, 22.71, 14.13.

Synthesis of **M**

A suspension of (E)-1-bromo-4-[2-(1-hexadecylpyrrole-2-yl)vinyl]-2,5-dioctyloxybenzene (**7**) (0.05 g, 0.069 mmol) and squaric acid (0.0039 g, 0.034 mmol) in a 1:1 *n*-butanol/toluene mixture (20 mL) was refluxed in a Dean-Stark apparatus for 3 h. The solvent was vacuum eliminated, and the residue was purified by column chromatography (silica gel, hexane/dichloromethane, 3:1) to afford the product as blue powder (0.021 g, 0.136 mmol, 45%): ¹H NMR (400 MHz, CDCl₃): δ = 0.86–0.93 (m, 18H), 1.09–1.58 (m, 104H), 1.79–1.93 (m, 12H), 4.03 (m, 8H), 4.82 (t, *J* = 12.8 Hz, 4H), 6.91 (d, *J* = 4.8 Hz, 2H), 7.01 (s, 2H), 7.13 (s, 2H), 7.27 (d, *J* = 16 Hz, 2H), 7.44 (d, *J* = 16 Hz, 2H), 7.87 (d, *J* = 2.8 Hz, 2H). ¹³C NMR (400 MHz, CDCl₃): δ = 168.71, 151.94, 149.89, 146.52, 130.55, 130.30, 125.19, 123.86, 123.06, 117.73, 116.70, 113.92, 113.75, 113.26, 70.45, 69.49, 46.69, 32.14, 31.91, 31.81, 31.78, 29.69, 29.53, 29.34, 29.24, 26.55, 26.10, 26.05, 22.66, 14.07.

N-(2-ethylhexyl)-2,7-bis (3-methyl-3-hydroxybut-1-ynyl)carbazole (**9**)

N-(2-ethylhexyl)-2,7-dibromocarbazole (0.437 g, 1 mmol) and 3-methyl-3-hydroxy-1-butyne (0.29 mL, 3 mmol) were dissolved in 15 mL triethylamine and 15 mL tetrahydrofuran. After a gentle stream of nitrogen was bubbled into the mixture for 1 h, Pd(PPh₃)₂Cl₂ (0.035 g, 0.05 mmol), PPh₃ (0.052 g, 0.2 mmol), and CuI (0.039 mg, 0.15 mmol) were added. The sample was refluxed for 6 h and then cooled to room temperature. After filtration, the solvent was vacuum eliminated, and the residue was purified by column

chromatography (silica gel, hexane/ethyl acetate, 2:1) to afford the product as white solid (0.23 g, 0.52 mmol, 52%): ^1H NMR (400 MHz, CDCl_3): δ = 7.89 (d, J = 8.0 Hz, 2H), 7.36 (s, 2H), 7.31 (d, J = 8.0 Hz, 2H), 4.04 (m, 2H), 1.98 (m, 1H), 0.79–0.85 (m, 6H). ^{13}C NMR (400 MHz, CDCl_3): δ = 140.03, 121.85, 121.39, 119.26, 118.86, 111.36, 92.43, 82.34, 64.76, 46.57, 38.12, 30.57, 29.74, 28.68, 27.53, 23.36, 22.03, 13.04, 9.93.

*N-(2-ethylhexyl)-2,7-diethynylcarbazole (**10**)*

A mixture of *N*-(2-ethylhexyl)-2,7-bis (3-methyl-3-hydroxybut-1-ynyl)carbazole (**9**) (0.44 g, 1 mmol) and NaH (0.072 g, 3 mmol) in 15 mL of toluene was heated refluxed under nitrogen with a vigorous stirring for 4 h. The reaction mixture was cooled, and then the solvent was removed and the crude product was purified by column chromatography on silica gel (petroleum ether) to give a white solid **9** (0.25 g, 0.75 mmol, 75%). ^1H NMR (400 MHz, CDCl_3): δ = 8.00 (d, J = 8.0 Hz, 2H), 7.53 (s, 2H), 7.36 (d, J = 8.0 Hz, 2H), 4.13 (m, 2H), 3.16 (s, 2H), 2.04 (m, 1H), 1.25–1.43 (m, 8H), 0.85–0.93 (m, 6H). ^{13}C NMR (400 MHz, CDCl_3): δ = 141.00, 123.24, 122.79, 120.47, 119.34, 113.04, 84.93, 47.59, 39.25, 30.86, 28.63, 24.37, 23.06, 14.17, 14.03, 10.91.

Synthesis of polymers

General procedure: To a 25 mL flask charged with the dibromo monomer **M** (0.2 mmol), diethynyl monomer (**4** or **5**) (0.2 mmol), $\text{Pd}(\text{PPh}_3)_4\text{Cl}_2$ (7 mg, 0.01 mmol), PPh_3 (13 mg, 0.05 mmol), and CuI (9.5 mg, 0.05 mmol), were added aqueous 2 M potassium carbonate (5 mL) and toluene (10 mL) under argon. The mixture was stirred and refluxed for 12 h. After being cooled to room temperature, the resulting solution was poured into methanol (300 mL). The precipitate was separated by filtration and washed with methanol. Soxhlet extraction was performed for 24 h with methanol and acetone, respectively.

P₁: dark powder, yield: 62%. IR (KBr pellet, cm^{-1}): 3444, 2923, 2852, 1625, 1460, 1386, 1205, 1100, 832, 701. ^1H NMR (400 MHz, CDCl_3): δ = 6.89–7.95 (m, 18H), 4.74 (m, 4H), 3.93 (m, 10H), 0.80–1.83 (m, 137H). ^{13}C NMR (400 MHz, CDCl_3): δ = 153.06, 150.56, 148.81, 145.47, 140.27, 133.83, 129.53, 122.04, 119.41, 119.28, 115.67, 112.74, 111.18, 85.61, 69.40, 68.97, 68.29, 45.76, 45.67, 38.22, 30.92, 30.01, 28.71, 28.36, 27.72, 25.58, 25.19, 23.08, 22.08, 21.67, 13.08, 9.97.

P₂: dark powder yield: 70%. IR (KBr pellet, cm^{-1}): 3442, 2922, 2853, 1628, 1506, 1464, 1382, 1264, 1111, 800, 561, 423. ^1H NMR (400 MHz, CDCl_3): δ = 8.07 (s, 2H), 6.86–7.79 (m, 12H), 4.76 (m, 4H), 4.02 (m, 12H), 1.15–2.10 (m, 128H), 0.78–0.82 (m, 24H). ^{13}C NMR

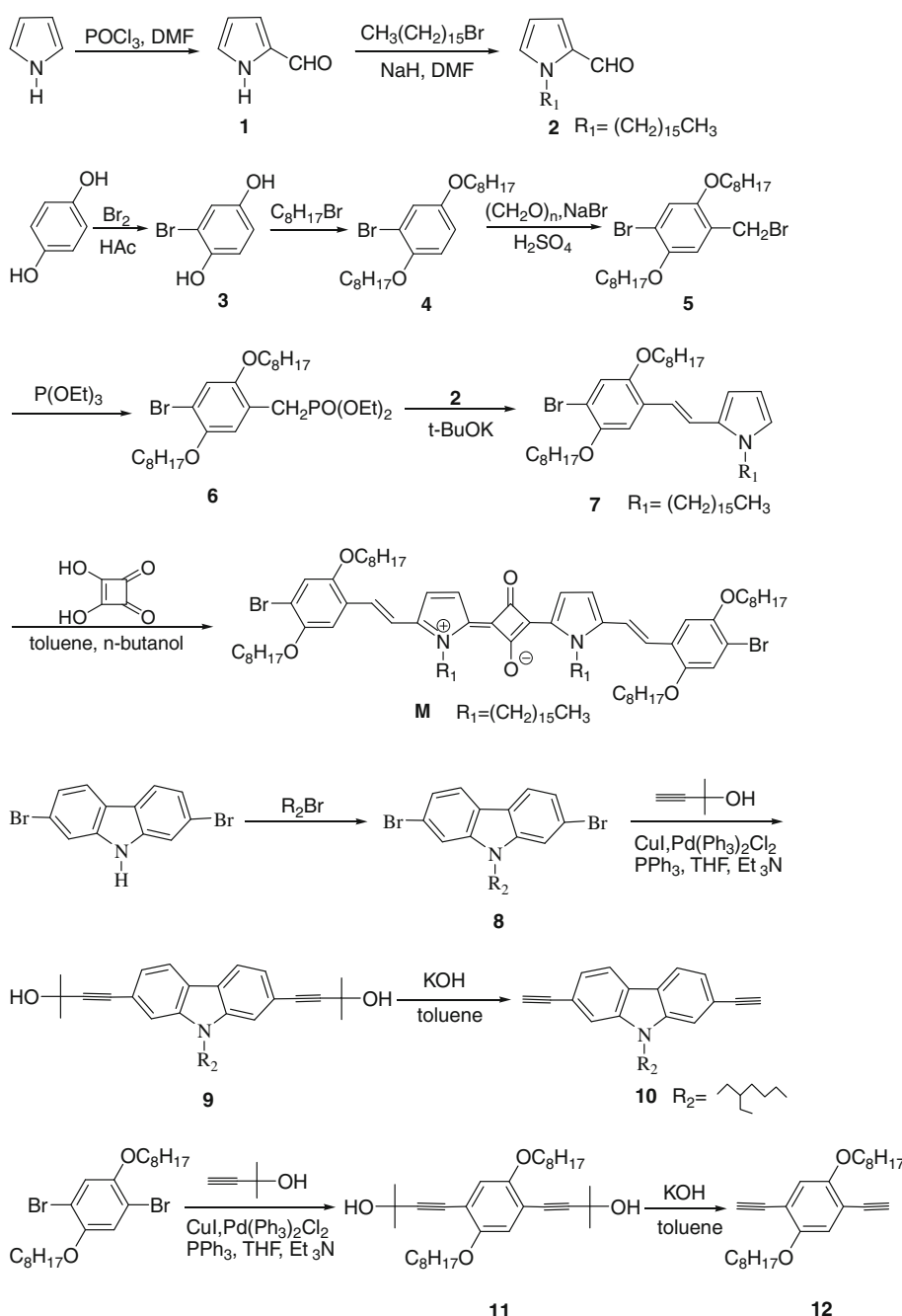
(400 MHz, CDCl_3): δ = 152.91, 152.64, 150.59, 134.19, 128.02, 127.21, 124.04, 116.30, 115.83, 112.99, 69.13, 68.75, 68.21, 52.89, 46.70, 45.77, 44.99, 41.32, 38.39, 38.08, 37.89, 36.42, 36.11, 35.72, 35.66, 35.28, 35.17, 35.00, 34.35, 33.84, 33.42, 32.73, 32.49, 32.07, 31.77, 30.93, 29.04, 28.70, 28.36, 26.98, 26.43, 26.09, 25.75, 25.48, 25.41, 25.21, 25.09, 23.80, 23.48, 21.69, 18.72, 13.09.

Results and discussion

Synthesis and characterization

The synthetic steps involved in the preparation of the monomers **2**, **7**, **M**, **10**, and **12** are outlined in Scheme 1. The intermediates **2**, **6**, and **12** were prepared following the already published procedures. The intermediate **7** was achieved through Wittig–Horner–Emmons reaction between 4-bromo-2,5-dioctyloxybenzylidethylphosphonate (**6**) and *N*-hexadecyl-pyrrole-2-carboxaldehyde (**2**) using *t*-BuOK in THF. The dibromo-substituted squaraine **M** was obtained with moderate yield through direct condensation of monomer **7** with squaric acid. Figure 1 gives the ^1H NMR and ^{13}C NMR spectra of the monomer **M**. Compound **8** was reacted with 3-methyl-3-hydroxy-1-butyne in a Sonogashira coupling to give **9** in about 50% yield. Subsequent deprotection with NaH led to monomer **10** in ~75% yield.

Copolymerizations leading to the final polymers **P₁** and **P₂** are presented in Scheme 2. The polymers were synthesized via palladium-catalyzed Sonogashira cross-coupling reaction [23, 24] in yields of over 60% with alkyl carbazole diacetylenes (**10**)/dialkoxyphenylene diacetylenes (**12**) and dibromo-substituted squaraine (**M**) as the starting materials. The weight-average molecular weights (M_w) measured by GPC against the standard of polystyrene and THF as eluent were about 89400 and 21500 with polydispersities (PDI) of 3.3 and 1.9 for **P₁** and **P₂**, respectively. The molecular weight of **P₁** is higher than **P₂**, which could be attributed to the side chains linked to **P₁** is different from that of **P₂**. The PDI of **P₁** is relatively high, and this may influence the flatness and compactness of the polymer film to some extent. These polymers showed high molecular weight, and the results are listed in Table 1. The obtained polymers were dark solids with good solubility in common organic solvents such as chloroform, THF, and toluene due to alkoxy and alkyl attached on the phenyl rings, pyrrole rings, and 9-position of carbazole units, respectively. In addition, the polymers could be readily processed into uniform thin film by casting or spin-casting from toluene solution, and were found to be air stable in both chloroform and solid state.

Scheme 1 Synthesis of the intermediate

The chemical structure of the polymers was characterized by FT-IR, ¹H NMR, and ¹³C NMR. ¹H NMR spectra of polymers **P**₁ and **P**₂ are shown in Fig. 2. The signals of the alkyl chain dominated in the region of δ = 0.78–2.10 ppm. The peaks at δ = 3.93 correspond to the hydrogen atoms of –OCH₂ and –NCH₂ linked to the phenyl or carbazole ring of **P**₁, and the signals of the –OCH₂ of alkoxy group of the phenyl appeared at δ = 4.03 ppm. The peaks at δ = 4.74 and 4.76 ppm could be assigned to the hydrogen atoms of –NCH₂ of pyrrole of **P**₁ and **P**₂, respectively. The signals of the vinylic unit and the phenyl were between δ = 6.86 and 8.07 ppm. Every peak in the ¹H-NMR spectra could be

assigned to the corresponding hydrogen atoms of the polymers. The polymers **P**₁ and **P**₂ were also characterized by FI-IR spectra which were shown in Fig. 3, strong absorptions were observed at 1625 and 1628 cm⁻¹ for **P**₁ and **P**₂, respectively, which were characteristic of the squaraine carbonyl.

Thermal properties

Thermal features of the polymers play a significant role in the preparation of actual OPV (organic photovoltaics) devices. The thermal properties of the polymers measured

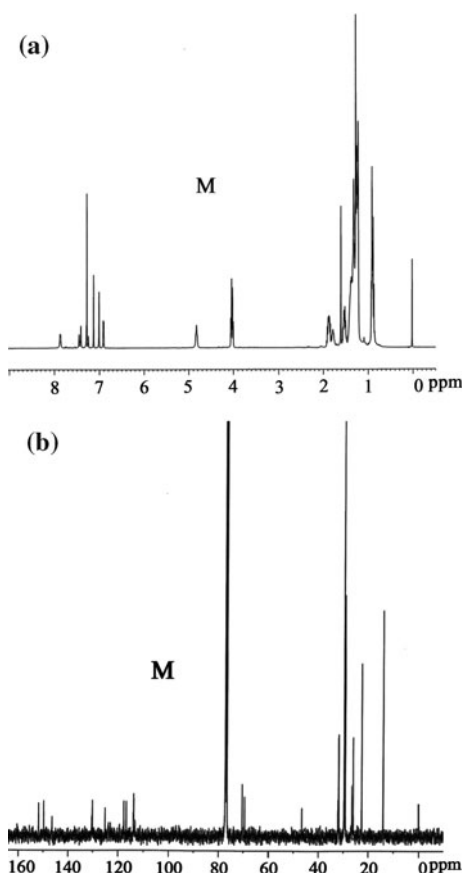


Fig. 1 **a** ^1H -NMR spectra of **M** and **b** ^{13}C -NMR spectra of **M**

Table 1 Yield, molecular weight, and thermal properties of the polymers

Polymer	Yield (%)	M_w^a	M_n^a	PDI (M_w/M_n) ^a	T_d^b (°C)	T_g (°C)
P₁	62	89400	27100	3.3	275	110
P₂	70	21500	11200	1.9	324	123

^a Molecular weights and polydispersity were measured by GPC, using THF as an eluent, polystyrene as a standard

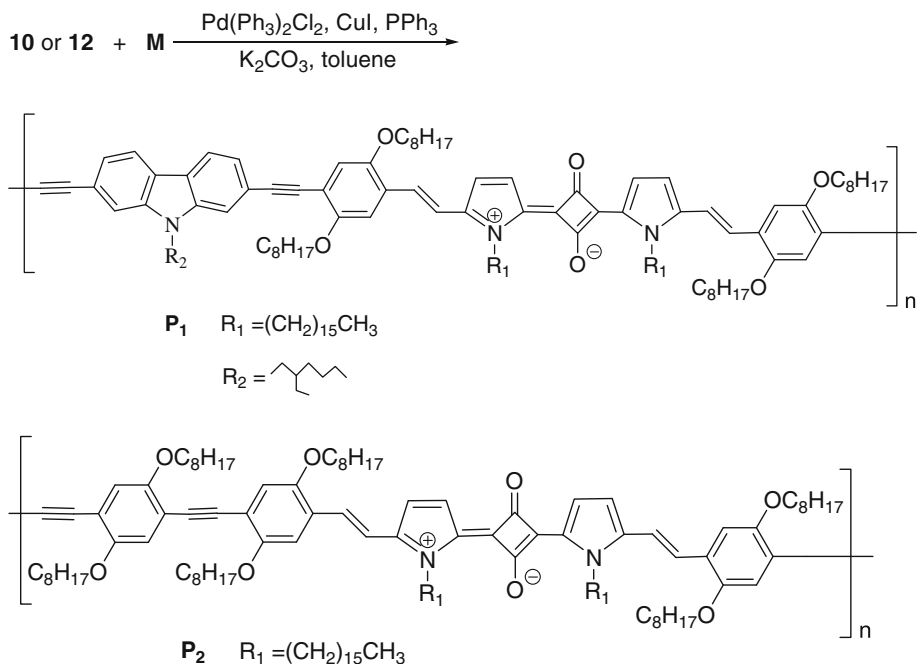
^b TGA curve of the polymers (the 5% weight-loss temperatures under nitrogen)

by TGA and DSC are summarized in Table 1. The sample holders were carefully weighed, and the samples were introduced. TGA was then carried out using heating rate at 10 °C min⁻¹ under nitrogen. As shown in Fig. 4, both polymers possessed good thermal stability. The onset points of the weight loss with 5% weight-loss temperature (T_d) of 275 and 324 °C for **P₁** and **P₂**, respectively, and no weight loss was observed at lower temperatures. The DSC curves of polymers are shown in Fig. 5. The glass transition temperatures of **P₁** and **P₂** are 110 and 123 °C, respectively. The thermal stability of the polymers is adequate for the fabrication processes of the photovoltaic devices.

Optical properties

The optical absorption spectra of the copolymers were measured in the dilute chloroform solution as well as in

Scheme 2 Synthesis of the copolymers



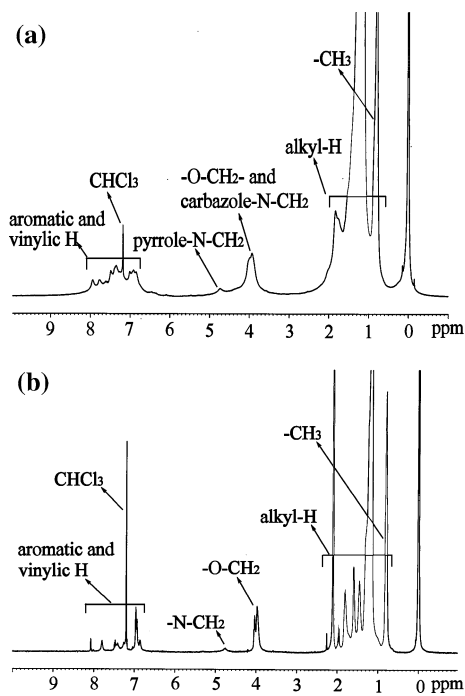


Fig. 2 ^1H -NMR spectra of **a** the polymer **P₁** and **b** the polymer **P₂**

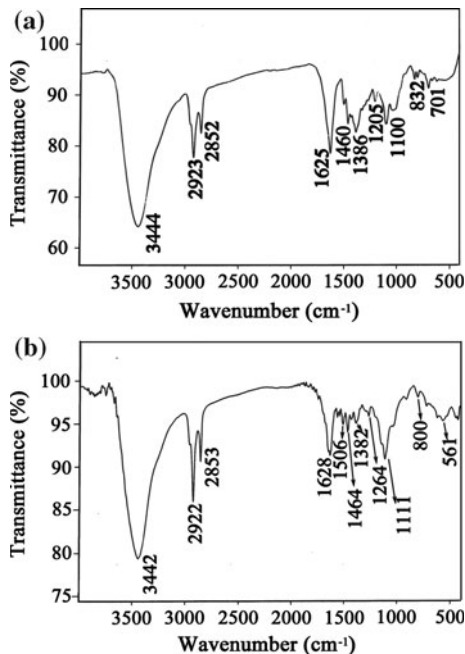


Fig. 3 FT-IR spectra of **a** the polymer **P₁** and **b** the polymer **P₂**

solid thin film as shown in Fig. 6. The dilute chloroform solution of each copolymer was filtered ($0.45 \mu\text{m}$ filter) to remove insoluble residue before the absorption spectrum was obtained. The main spectroscopic data of the polymers are summarized in Table 2. In solution, **P₁** and **P₂** show similar absorption spectra and both have two distinct absorption bands with the maximum peaks of 741 and

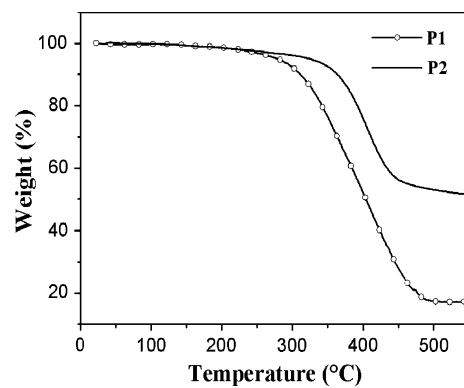


Fig. 4 TGA thermograms of the polymers

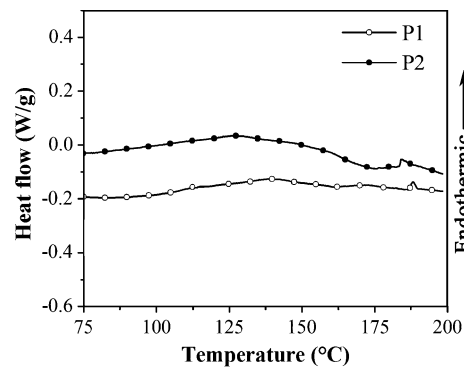


Fig. 5 DSC thermograms of the polymers

749 nm for **P₁** and **P₂**, respectively. The former band can be assigned to $\pi-\pi^*$ transition whereas the latter band may be due to ICT interactions resulted from the alternating donor–acceptor structure in the polymer [25]. The copolymers exhibit lower energy absorption peaks than **M** (708 nm), diethyl-PPE [26] (379 nm in chloroform), and poly(*N*-arylcarbazole-2,7-ylene) [27] (~ 380 nm in chloroform), and the red-shifts of **P₁** and **P₂** may be resulted of the presence of the charge-transferred (CT) electronic state in these copolymers. Such CT actions could be attributed to the formation of the conjugated system between the electron-accepting squaraine units and electron-donating alkyl carbazole/dialkoxyphenylene units.

Thin films of the copolymers were obtained by spin-coating on quartz substrates from their chloroform solution. Usually, the solid-state absorption spectra of the polymers are more or less similar to their solution spectra; however, interestingly, the absorption spectra of **P₁** and **P₂** in the solid state are quite different from that in solution, and the absorption bands of the resulted polymers are apparently broadened in film in comparison to the sharp absorption in solution. The maximum absorbance of the films of **P₁** and **P₂** are 796 and 851 nm, respectively, and there are 55 and 102 nm red-shifts for **P₁** and **P₂** compared with their absorbance in chloroform. The broadened absorption and

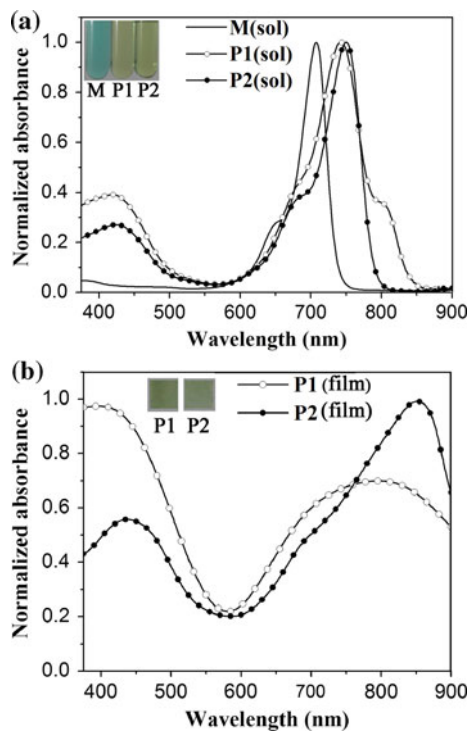


Fig. 6 UV-Vis absorption spectra of the polymers solutions in CHCl_3 and films on a quartz plate **a** the pictures of polymer solutions and **b** the pictures of polymer films)

large red-shifts indicate higher coplanarity of the polymers as well as a more specific and ordered packing of the aggregates of the polymer chains in the solid film [28]. The optical band gaps (E_g^{opt}) of the polymers, derived from the absorption edge of the thin film spectra which are over 900 nm, are lower than 1.38 eV.

Electrochemical properties

Cyclic voltammetry (CV) was employed to investigate the oxidation/reduction properties of the polymers, and estimate the HOMO and LUMO energy levels of the materials as well. CV has been carried out using thin films of polymers prepared from chloroform (5 mg mL^{-1}) in anhydrous acetonitrile at a scan rate of 100 mV s^{-1} and SCE serves as the reference electrode. Figure 7 shows the CV of polymers, and Table 2 summarizes the electrochemical properties of **P₁** and **P₂**. The onset oxidation potentials

($E_{\text{onset,ox}}$) for **P₁** and **P₂** occur at 0.66 and 0.57 V, respectively. The corresponding onset reduction potentials ($E_{\text{onset,red}}$) appear at -0.79 and -0.85 V, respectively. The HOMO and LUMO energy levels of the polymers could be calculated from the onset oxidation potentials and the onset reduction potentials of the polymers, according to the following equations [29].

$$I_p(\text{HOMO}) = -(E_{\text{onset,ox}} + 4.39)\text{eV}$$

$$E_a(\text{LUMO}) = -(E_{\text{onset,red}} + 4.39)\text{eV}$$

$$E_g^{\text{el}} = E_{\text{onset,ox}} - E_{\text{onset,red}}$$

Therefore, the LUMO and HOMO energy levels of the polymers are -3.60 , -3.54 eV and -5.05 , -4.96 eV for **P₁** and **P₂**. The electrochemical band gaps (E_g^{el}) are estimated to be 1.45 and 1.42 eV for polymers **P₁** and **P₂** from the above equation. It implies that the energy gaps of the polymers were reduced through forming donor–acceptor structure. The higher HOMO level of the polymer **P₂** indicates the stronger ICT effects [30]. Their E_g^{el} are larger than the optically determined ones ($E_g^{\text{opt}} < 1.38$ eV). The difference between optical and electrochemical band gap energies can be explained in part by the exciton binding energy of conjugated polymers which is believed to be in the range of ~ 0.4 – 1.0 eV [23].

Conclusions

Two novel donor–acceptor conjugated PAEs consisting of squaraine as the electron-accepting building block and alkyl carbazole/dialkoxyphenylene as bridging unit have been synthesized through palladium-catalyzed Sonogashira cross-coupling reactions. These copolymers exhibit good solubility in common organic solvents such as CHCl_3 , THF, and toluene and were found to be both air stable and thermally stable, which may improve the operating lifetime of the solar cells. The electrochemical and photophysical properties were investigated, and the results show that the incorporation of squaraine to the main chains of the polymers could reduce the energy band gaps and improve the near IR absorption properties effectively. These properties suggest that the polymers might be useful for photovoltaic device applications and the devices which have the general

Table 2 Optical and electrochemical properties of the polymer **P₁**, **P₂**

Polymer	$\lambda_{\text{max,sol}}^{\text{a}}$ (nm)	$\lambda_{\text{max,film}}$ (nm)	$E_{\text{onset,ox}}^{\text{b}}$ (V)	$E_{\text{onset,red}}^{\text{b}}$ (V)	HOMO (eV)	LUMO (eV)	E_g (eV)
P₁	419, 741	397, 796	0.66	-0.79	-5.05	-3.60	1.45
P₂	426, 745	437, 851	0.57	-0.85	-4.96	-3.54	1.42

^a ca. 10^{-5} mol L^{-1} in CHCl_3 , wavelength of maximum

^b Oxidation and reduction onset potential measured by cyclic voltammogram (vs. SCE)

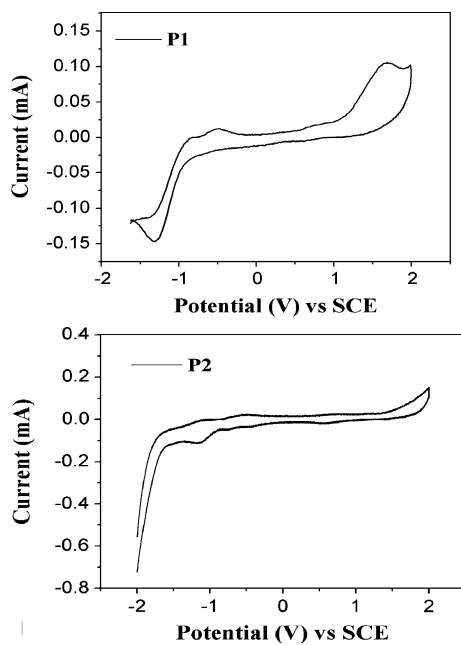


Fig. 7 Cyclic voltammogram of the polymers **P₁** and **P₂**

structure of ITO/PEDOT:PSS/polymer:fullerene/LiF/Al are now in progress.

Acknowledgements This study was supported by the key foundation of education ministry of China (20070610053) and Sichuan Province Foundation for Youths (2008JY0050). The authors also acknowledge the Analytical & Testing Center of Sichuan University for the NMR measurements.

References

1. Schmidt-Mende L, Fechtenkotter A, Mullen K (2001) *Science* 293:1119
2. Goris L, Haenen K, Nesladek M (2005) *J Mater Sci* 40:1413. doi: [10.1007/s10853-005-0576-0](https://doi.org/10.1007/s10853-005-0576-0)
3. Chen JW, Cao Y (2009) *Acc Chem Res* 42:1709
4. Qiao F, Liu A, Zhou Y (2009) *J Mater Sci* 44:1283. doi: [10.1007/s10853-009-3280-7](https://doi.org/10.1007/s10853-009-3280-7)
5. Thompson BC, Frechet JMJ (2008) *Angew Chem Int Ed* 47:58
6. Dennler G, Scharber MC, Brabec CJ (2009) *Adv Mater* 21:1323
7. Kim JY, Lee K, Coates NE, Moses D, Nguyen TQ, Dante M, Heeger AJ (2007) *Science* 317:222
8. Liang YY, Xu Z, Xia JB, Tsai ST, Wu Y, Li G, Ray C, Yu LP (2010) *Adv Mater* 22:1
9. Bunz UHF (2009) *Macromol Rapid Commun* 30:772
10. Ashraf RS, Shahid M, Klemm E, Al-Ibrahim M, Sensfuss S (2006) *Macromol Rapid Commun* 27:1454
11. Ashraf RS, Klemm E (2005) *J Polym Sci Part A Polym Chem* 43:6445
12. Bagnis D, Beverina L, Huang H, Silvestri F, Yao Y, Yan H, Pagani GA, Marks TJ, Facchetti A (2010) *J Am Chem Soc* 132:4074
13. Geiger T, Kuster S, Yum J, Moon S, Nazeeruddin M, Grätzel M, Nüesch F (2009) *Adv Funct Mater* 19:2720
14. Eldo J, Ajayaghosh A (2002) *Chem Mater* 14:410
15. Ajayaghosh A (2003) *Chem Soc Rev* 32:181
16. Roncali J (1997) *Chem Rev* 97:173
17. Brédas JL (1985) *J Chem Phys* 82:3808
18. Hunt JT, Mitt T, Borzilleri R, Gullo-Brown J, Farnoli J, Fink B, Han WC, Mortillo S, Vite G, Wautlet B, Wong T, Yu C, Zheng XP, Bhide R (2004) *J Med Chem* 47:4054
19. Aldabbagh F, Bowman WR, Mann E (1997) *Tetrahedron Lett* 38:7937
20. Egbe DAM, Bader C, Klemm E, Ding LM, Karasz FE, Grummt UW, Birckner E (2003) *Macromolecules* 36:9303
21. Tsai HC, Yu IC, Chang PH, Yu DC, Hsieh GH (2007) *Macromol Rapid Commun* 28:334
22. Chi JH, Park SH, Lee CL, Kim JJ, Jung JC (2007) *Macromol Mater Eng* 292:844
23. Dieck HA, Heck RF (1975) *J Organomet Chem* 93:259
24. Sonogashira K, Tohda Y, Hagihara N (1975) *Tetrahedron Lett* 16:4467
25. Wu PT, Kim FS, Champion RD, Jenekhe SA (2008) *Macromolecules* 41:7021
26. Zou YP, Tan ZA, Huo LJ, Li YF (2008) *Polym Adv Technol* 19:865
27. Kijima M, Koguchi R, Abe S (2005) *Chem Lett* 34:900
28. Chen H, Cai XR, Xu ZG, Zhang T, Song BF, Li Y, Jiang Q, Xie MG (2008) *Polym Bull* 60:581
29. Bredas JL, Silbey R, Boudreux DS (1983) *J Am Chem Soc* 105:6555
30. Tsai JH, Chueh CC, Lai MH (2009) *Macromolecules* 42:1897